01 Nov 1974

Molecular Model for Ice Clusters in a Supersaturated Vapor

Barbara N. Hale
Missouri University of Science and Technology, bhale@mst.edu

P. L. M. Plummer
Missouri University of Science and Technology

Recommended Citation

Molecular model for ice clusters in a supersaturated vapor*

B. N. Hale and P. L. M. Plummer

Department of Physics and Graduate Center for Cloud Physics Research, University of Missouri-Rolla, Rolla, Missouri 65401
(Received 15 July 1974)

A molecular model previously applied to prenucleation water clusters is used to examine ice I_h embryos. The canonical partition function is evaluated for clusters having from 6 to 64 water molecules. The intermolecular vibrational free energies are extrapolated to clusters containing up to 120 molecules and free energies of formation, nucleation rates, and critical supersaturation ratios are calculated and compared with experiment. For the clusters studied, the ice I_h structure appears to be much less stable at all temperatures than the more spherical clathratelike cluster.

I. INTRODUCTION

In previous papers[1,2] we presented a molecular model for prenucleation water clusters[1] and compared the calculated homogeneous nucleation rates[2] with those obtained experimentally and those calculated from classical theories. In this paper, we would like to describe the model in detail and apply it to icelike clusters in a supersaturated vapor. The difficulties associated with nucleating ice from a pure vapor are well known.[3] However nucleation of ice in the atmosphere is central to many atmospheric processes. While the latter is not a homogeneous nucleation process, it is useful to examine ice nucleation from a pure vapor in order to gain insight into the nucleation process and the growth of the embryos.

In Sec. II we describe the molecular model in detail. The model has been extended (since our first application of it to clathrate clusters[1]) and, in particular, includes configurational entropy contributions to the partition function. The model is applied to ice I_h clusters, and the evaluation of the partition function is explicitly described. The free energies of formation are also calculated in Sec. II. A comparison is made with the clathrate model[1] and with a simple spherical cluster model using ice surface tension. In Sec. III we review the steady-state nucleation formalism and describe how the energies of formation are used to calculate the nucleation rate and the critical supersaturation ratios. We compare the latter to experiment and other models. In Sec. IV we discuss the implications of these results.

II. THE MODEL: CLUSTER STRUCTURE, THE PARTITION FUNCTION, AND THE FREE ENERGIES OF FORMATION

The importance of using a molecular model for water clusters rather than a macroscopic model using surface tension and other bulk properties has already been discussed.[1] We begin, therefore, with the molecular model itself. The quantity to be calculated is the concentration of clusters with n molecules, N_n, in the vapor at temperature, T, and with supersaturation ratio, S. We make the conventional assumption that the cluster–vapor system is a mixture of noninteracting ideal gases. Therefore, the size concentration is given by[1]

$$N_n = Z(n)[N_1/Z(1)]^n, \tag{1}$$

where $Z(n)$ is the canonical partition function for a cluster with n water molecules. The molecular properties of water in specific cluster structures are calculated and used to obtain $Z(n)$.

One of the basic assumptions of our model is that the Hamiltonian for the n-molecule cluster can be written as a sum of separate terms,

$$H(n) = H_T + H_R + H_V + H_B, \tag{2}$$

where H_T and H_R are the rigid body translational and rotational energy operators for the cluster; H_V represents the vibrational energy internal to the cluster and H_B the intermolecular binding energy. The partition function is given by

$$Z(n) = \sum_i \exp[-\langle i| H(n)| i\rangle/kT], \tag{3}$$

where the summation i is over all possible states of the system. Using Eq. (2) we write

$$Z(n) = Z_T Z_R Z_V Z_B Z_C, \tag{4}$$

where Z_C represents the contribution from configurational entropy. This will be described later. The rigid body translational and rotational partition functions are given by[1]

$$Z_T(n) = V(2\pi mnkT/h^2)^{3/2} \tag{5a}$$

and

$$Z_R(n) = \pi^{1/2}(8\pi^2 kT/h^2)^{3/2}(I_1 I_2 I_3)^{1/2}\delta^{-1}, \tag{5b}$$

where I_1, I_2, and I_3 are the principal moments of inertia of the n cluster and δ is the rotational symmetry number and are dependent on the structure of the cluster.

In order to evaluate the moments of inertia and $Z_V(n)$, $Z_B(n)$, and $Z_C(n)$, we must assume the cluster of n molecules has a well-defined structure. Thus the second basic assumption is that a specific structure for the n cluster exists and represents the time average of the quasiequilibrium n cluster in the supersaturated vapor. This treatment of the partition function assumes that the cluster structure has a lifetime sufficiently long that its internal vibrational spectrum can be characterized. In the discussion that follows the structures chosen for investigation have an ice I_h structure composed of rings containing six water molecules. A typical structure with 20 molecules is shown in Fig. 1. As before,[1] we assume the internal structure of the water molecule is only slightly affected by cluster formation.

The binding energy contribution to the partition func-

TABLE I. The bond energies, intramolecular, and librational frequencies are shown as a function of the number of hydrogen bonds attached to a given water molecule in the cluster.

	Monomer	1 bond	2 bonds	3 bonds	4 bonds
E_i (kcal/mol)	⋯	6.10	6.28	6.36	6.40
Intra (cm⁻¹)	3750	3695	3690	3565	3565
	3650	3545	3555	3470	3470
	1590	1645	1650	1655	1655
Libr (cm⁻¹)	⋯	624	600	536	608
		480	464	480	512
		384	312	384	456

tion, Z_B, is assumed to be

$$Z_B(n) = \exp[-E_B(n)/kT], \tag{6}$$

where the intermolecular binding energy, $E_B(n)$, of the n cluster is

$$E_B(n) = \tfrac{1}{2}(n_1 E_1 + 2n_2 E_2 + 3n_3 E_3 + 4n_4 E_4). \tag{7}$$

In the above equation, n_i is the number of i-bonded molecules in the n cluster. Each E_i is an average hydrogen bond energy associated with bonds surrounding an i-bonded molecule. These E_i are the results of INDO[4] calculations on small water clusters containing two to five water molecules.[5] In Table I are the E_i obtained for the four different bonding configurations used in these studies.

The vibrational partition function, $Z_V(n)$, is assumed to be factorable as follows:

$$Z_V(n) = Z_{\text{intramolecular}} Z_{\text{librational}} Z_{\text{intermolecular}}. \tag{8}$$

This was described in detail in Ref. 1. This approximation is consistent with the wide separation in the frequency bands associated with the three different types of molecular motion as is illustrated in Fig. 2. For each molecule there are three intramolecular frequencies and three librational frequencies. The number of intermolecular frequencies for an n cluster is $3n-6$. As is the case for the total binding energy of the cluster, the intramolecular and librational partition functions must reflect the environment of the individual mole-
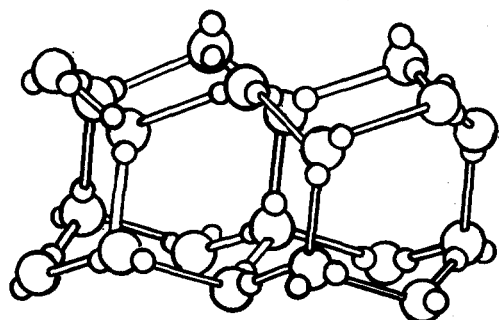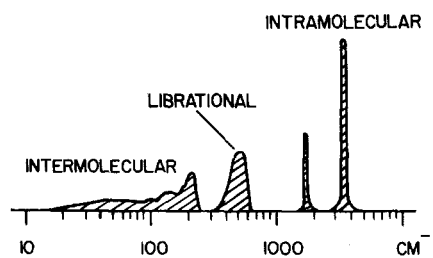

FIG. 2. The approximate range of the intermolecular, librational, and intramolecular vibrational bands for small water clusters.

cules. This was done by assuming the form in Eq. (9) for $Z_{\text{intramolecular}}$ and $Z_{\text{librational}}$. Specific frequencies are associated with an i-bonded molecule and the partition function is weighted with respect to n_i, the number of such molecules,

$$Z_{\substack{\text{intramolecular} \\ \text{(or librational)}}}(n) = \prod_{i=1,4} Z_{i \substack{\text{intramolecular} \\ \text{(or librational)}}}^{n_i}. \tag{9a}$$

Each Z_i is the partition function for a harmonic oscillator with three normal modes:

$$Z_i = \prod_{j=1,3} \frac{\exp(-ch\nu_{ij}/2kT)}{1 - \exp(-ch\nu_{ij}/kT)}. \tag{9b}$$

The wavenumbers ν_{ij} used in Eq. (9b) are given in Table I. The procedure for determining the ν_{ij} is described in Refs. 1 and 6.

The intermolecular vibrational partition function for $3N-6$ normal modes is

$$Z_{\text{intermolecular}}(n) = \prod_{j=1}^{3n-6} \frac{\exp(-ch\nu_j/2kT)}{1 - \exp(-ch\nu_j/kT)}. \tag{10}$$

The ν_j are calculated directly for the smaller ice clusters (with less than 65 molecules) treating the molecules as point masses and using conventional normal mode techniques.[7] The intermolecular potential was taken as

$$2V = k_r \sum_{ij} r_{ij}^2 + k_\alpha r_e^2 \sum_{ijk} \alpha_{ijk}. \tag{11}$$

The force constants used are those for ice[8]: 0.19 mdyn Å⁻¹ for k_r and 0.00475 mdyn Å⁻¹ for k_α, where α_{ijk} is the angle between molecules i, j, and k, where i and k are nearest neighbors to j; and r_e is the equilibrium nearest neighbor distance. References 1 and 6 discuss these calculations in more detail. Figure 3 illustrates the distribution of the calculated intermolecular frequencies for representative clusters with 6–64 molecules compared with bulk ice.[9]

For clusters with more than 64 molecules the intermolecular contribution to the free energy is extrapolated from the results for the 48 and 64 cluster using the following form for $F_{\text{inter}}(n)$:

$$\frac{F_{\text{inter}}(n)}{kT} = n\left(\frac{E}{kTn} - \frac{S_e}{kn}\right). \tag{12}$$

The total intermolecular vibrational energy, E, approaches $3nkT$ very rapidly with increasing n as is shown in Fig. 4. However, the intermolecular vibra-

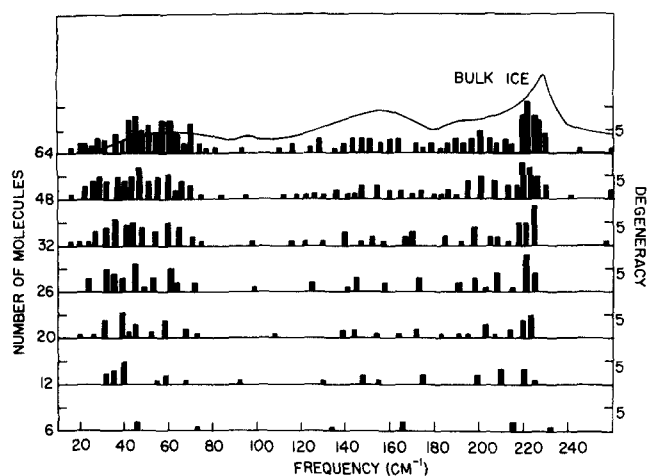FIG. 1. The 20-molecule ice I_h structure.

FIG. 3. The distribution of calculated intermolecular vibrational frequencies for small ice I_h clusters. The density of states for ice I_h is taken from Bertie and Whalley.[9]

tional entropy S_e is much more sensitive to the cluster shape and molecular environment[10] as well as to the surface to volume ratio. The latter approaches the bulk value only for very large clusters $(n > 10^4)$. Values of $F_{inter}(n)$ for $n > 64$ are obtained by setting $E = 3nkT$ and approximating the entropy per molecule (in units of k) by

$$\frac{S_e}{kn} = \frac{S_e^0}{k}\left(\frac{n_2 + n_3}{n}\right) + \frac{S_e^{bulk}}{kn}\left(\frac{n_4}{n}\right). \qquad (13)$$

This form for the entropy approaches the bulk value as the fraction of surface molecules, $(n_2 + n_3)/n$, goes to zero and is equal to the exact calculated value of the entropy at $n = 64$ and $n = 48$. The exact value at $n = 64$ determines S_e^0. The dashed lines in Fig. 4 show the extrapolations for large ice I_h clusters. However, only a small portion of the extrapolated entropy curve (that for $n \le 120$) is used in our nucleation rate and critical supersaturation ratio calculations. In most cases the critical sized cluster has fewer than 100 molecules. The value for the intermolecular entropy per molecule for bulk ice, $S_e^{bulk}/kn = 4.0$, was chosen on the basis of three independent estimates: (1) from the specific heat calculations of Giauque and Stout,[11] (2) from the intermolecular vibrational density of states of Bertie and Whalley[9]; and (3) from the entropy per molecule of bulk water[12] with the entropy of fusion and librational contributions subtracted.

The configurational contribution to the partition function, $Z_C(n)$, has two sources: (1) $\Omega(n)$, the number of ways the specific n cluster can be constructed by interchanging molecules and hydrogens along the bonds, and (2) the sum over contributions from other n clusters having a different number of bonds and/or a different geometrical structure. To illustrate this, we return to Eq. (4) and rewrite $Z(n)$ as follows:

$$Z(n) = (Z_T Z_R Z_V Z_B)_I \Omega_I(n)\left(1 + \sum_j \frac{(Z_T Z_R Z_V Z_B)_j \Omega_j(n)}{(Z_T Z_R Z_V Z_B)_I \Omega_I(n)}\right). \qquad (14)$$

Here the subscript I refers to the lowest energy ice I_h structure and j to other ice structures with n molecules. The configurational partition function, $Z_C(n)$, is then defined as follows:

$$Z_C(n) \equiv \Omega_I(n)\left[1 + \sum_j \exp\left(\frac{F_I(n)}{kT} - \frac{F_j(n)}{kT}\right)\right], \qquad (15)$$

where

$$F_j(n) = -kT \ln[(Z_T Z_R Z_V Z_B)_j \Omega_j(n)] \qquad (16)$$

is the Helmholtz free energy of the j cluster. In a general application of the molecular model, I is the structure giving the major contribution to the sum in Eq. (3). It may be viewed as the time average of a collection of n clusters or as the structure which has a significantly low energy of formation and small entropy. The contribution from the sum over j becomes more apparent when one views the I structure as having the lowest Helmholtz free energy and defines a new quantity

$$\Delta_{Ij}(n) = [F_I(n)/kT - F_j(n)/kT].$$

$\{\Delta_{Ij}(n)$ is also the difference in the Helmholtz free energies of formation[see Eq. (20)] of the I and j structures$\}$. Suppose there are M_l (different) structures with Helmholtz free energies approximately equal to $F_l(n)$. Then Z_C can be approximated by

$$Z_C(n) \simeq \Omega_I(n)\left[1 + \sum_l M_l \, e^{\Delta_{Il}(n)}\right]. \qquad (17)$$

Since the I structure has, by definition, the lowest Helmholtz free energy, $\Delta_{Il}(n)$ is negative for all l. Thus the summation over l can only alter $Z_C(n)$ when M_l is sufficiently large. For example if $\Delta_{Il} = -6$ (approximately one-half of a single hydrogen bond energy) then M_l must be 10^5; if $\Delta_{Il} = -1$ then M_l need only be about 200. These combinations of Δ_{Il} and M_l would produce a $5kT$ reduction in the Helmholtz free energy of formation and could produce no more than two orders of magnitude increase in the nucleation rate, J. Based on this analysis, our previous results[2] (using clathrates with five-membered rings as the I structure) would be unchanged by the consideration of ice I_h structures (where $\Delta_{Il} \approx -25$) or clathrates with one or more completely broken bonds $(\Delta_{Il} < -12)$. Figure 6 of Ref. 2 illustrates
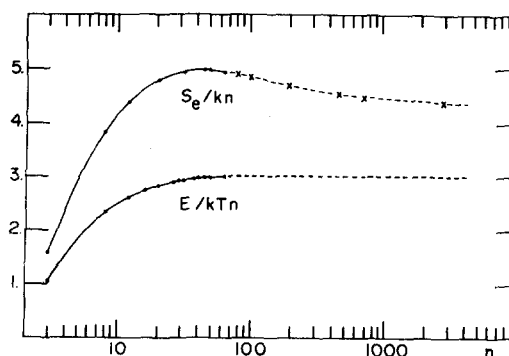

FIG. 4. The solid lines are the calculated intermolecular energy and entropy per molecule vs cluster size at $T = 273$ K. The dashed curves are extrapolated. Equation (13) is used for the extrapolation of the entropy of large clusters.
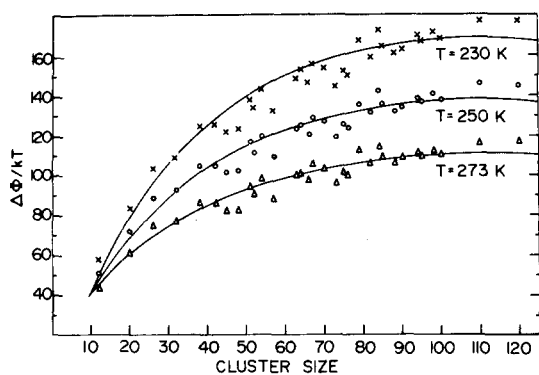
FIG. 5. The points are calculated $\Delta\phi(n)/kT$ vs cluster size n for $S=5$ and $T=230$, 250, and 273 K. The solid lines are fits of the form $An^{2/3} - Bn + c$.

the large magnitude of Δ_{II} for ice I_h structures.

In the present work, the only cluster structures considered are the ice I_h structures, and these were chosen in order to evaluate the nucleation rate and critical supersaturation of ice in the vapor. Hence, the I structure is the maximally bonded n-ice cluster. The sum over j then reduces to a sum over geometrically different ice I_h structures (e.g., a two-layered structure rather than a more compact three-layered structure) and a sum over broken-bonded or deformed ice I_h clusters. Structures with completely broken bonds and those with fewer bonds than the most compact structure give a negligible contribution to $Z_C(n)$. The deformed ice I_h structures we neglect in this particular case because of our original intent to look only at pure ice I_h.

The contribution to the residual entropy, $\Omega_I(n)$, must be included. Determining the number of ways to build a specific structure from n polyatomic molecules is not an easy task—especially for large n. In the present results we use the following simple form:

$$\Omega_I(n) = (n! / \pi_i n_i!)(2)^{N_B(n)}. \tag{18}$$

In Eq. (18), $N_B(n)$ is the number of bonds in the n cluster and n_i is the number of i-bonded molecules. The expression in Eq. (18) gives an upper limit for the number of ways one can build an ice I_h n cluster with N_B bonds. A smaller residual entropy is obtained from a more careful consideration of the positions of the hydrogens along the bonds. This procedure would overestimate the entropy for very large clusters but should be quite reasonable for the cluster sizes considered here.

The "free energy of formation," $\Delta\phi(n)/kT$, is obtained from Eq. (1),

$$N_n = Z(n)\left(\frac{N_1}{Z(1)}\right)^n \equiv N_1^0 \exp\left(-\frac{\Delta\phi(n)}{kT}\right), \tag{19}$$

where N_1^0 is the equilibrium number of monomers in the vapor at temperature T. Thus $\Delta\phi(n)/kT$ is

$$\Delta\phi(n)/kT = -\ln[Z(n)/N_1^0] + n\ln[Z(1)/N_1^0] - n\ln S, \tag{20}$$

where S, the supersaturation ratio, is N_1/N_1^0. After

evaluating $Z(n)$ as described for a range of cluster sizes, we obtain the free energy of formation for ice I_h as shown in Fig. 5 for $S=5$ and $T=230$ K, 250 K, and 273 K. The solid lines are fits (discussed in Sec. III) to the somewhat scattered points for $\Delta\phi(n)/kT$ assuming a form $An^{2/3} - Bn + C$. One expects the free energy of formation to approach a smooth function of n for large n. The scatter in the points can be reduced by searching for more compact structures (those having more bonds) or by a more precise determination of $\Omega(n)$. The balance between binding energy and entropy should serve to smooth out the free energy of formation as a function of n.

III. PROCEDURE FOR CALCULATING NUCLEATION RATES

In order to calculate nucleation rates from the vapor using a molecular model, we assume the following steady state nucleation rate[2,13]:

$$J = \left(\sum_n \frac{1}{C_n N_n}\right)^{-1}, \tag{21}$$

where N_n is the quasiequilibrium concentration of n clusters, defined in Eq. (19), and C_n is the rate at which monomers are absorbed by an n cluster. For C_n we have used the classical expression,

$$C_n = N_1 \bar{v} A(n) \alpha, \tag{22}$$

where $A(n)$ is the average surface area of the n cluster, $\bar{v}$ is $(kT/2\pi M)^{1/2}$, M is the mass of a water molecule, and α is the probability that a monomer striking the surface will be adsorbed. For these results we have used $\alpha = 1$ which gives an upper limit for C_n.[14]

To calculate the steady state nucleation rate, J, a least squares fit is made to the points for $\Delta\phi(n)/kT$ using an expression of the form

$$\Delta\phi(n)/kT = An^{2/3} - Bn + C. \tag{23}$$

This form was chosen because its functional dependence on n is identical to that of the classical spherical cluster model. The steady state nucleation rate is not sensitive to the functional form for $\Delta\phi/kT$ but rather depends on the magnitude and corresponding n value of the relative maximum.[15] The n value for which $\Delta\phi/kT$ is a maximum is defined to be $n*$, the number of molecules in the critical size cluster. The least squares fits are also shown in Fig. 5.

Using Eq. (23) for $\Delta\phi/kT$, we find[2]

$$n* = (2A/3B)^3, \tag{24}$$

$$\Delta\phi(n*)/kT = Bn*/2 + C, \tag{25}$$

and

$$J = C_{n*} N_1^0 \exp[-\Delta\phi(n*)/kT]\gamma_{n*}. \tag{26}$$

The last factor in Eq. (26), γ_{n*}, is[16]

$$\gamma_{n*} = \left(\frac{\Delta\phi(n*)/kT}{3n*^2}\right)^{1/2}. \tag{27}$$
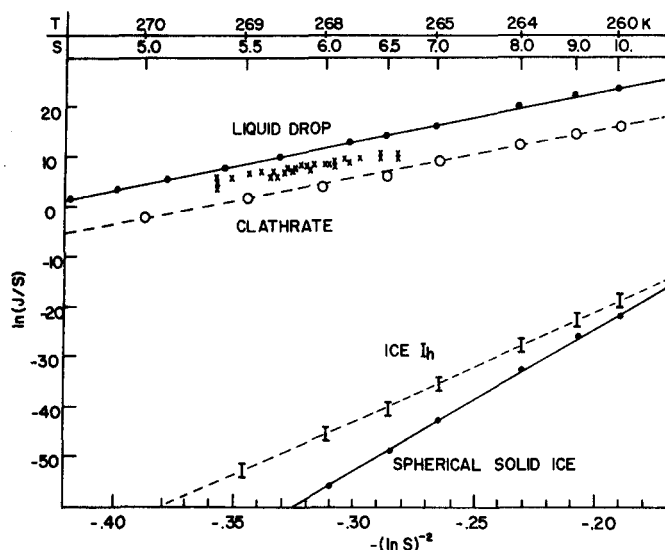
FIG. 6. The calculated $\ln(J/S)$ vs $(-\ln S)^{-2}$ for the ice I_h and clathrate molecular models are compared with some experimental data from Biermann[17] and Kassner[18] (×). Two classical model calculations are also shown. The spherical ice cluster model assumes an ice–vapor surface tension of $141-0.15T$ erg/cm^2. The starting temperature for the experimental points is 25 °C.

The expression for J in Eq. (26), using $\Delta\phi/kT$ as given in Eq. (23), approximates the sum given in Eq. (21) to within 1% or 2%—an amount much less than the uncertainties in the energies of formation or in the experimental data for J. In Fig. 6 we show the nucleation rate calculations for the ice I_h clusters and compare these with some experimental homogeneous nucleation rates measured by Biermann[17] and Kassner[18] in an expansion cloud chamber. Instead of plotting $\ln J$ vs S, we have plotted $\ln(J/S)$ vs $-(\ln S)^{-2}$ which, according to Eqs. (23)–(27), should yield a straight line for constant T. This can be seen in Fig. 6 where quantities are plotted for the models and for the experimental data. Actually, the temperature varies slightly over the range of experimental points since the run corresponds to a fixed initial temperature (before expansion of the chamber). The final temperatures for the calculations range from 270 K at $S=5.0$ to 260 K at $S=10.0$. This temperature variation produces some deviation from the linear relationship. The experimental data have a much smaller temperature variation and are consistent with the linear relationship. However, we have not drawn a line through the points since it is not clear how much the nucleation rate falls off, due to vapor depletion at the higher supersaturations. No experimental data were available for S larger than 6.5, but we have extended the model calculations to higher supersaturation ratios and lower temperatures.

To illustrate the lower relative stability of the ice I_h clusters as opposed to the clathrate clusters studied previously,[1,2] we include in Fig. 6 the clathrate cluster model results. Small clathrate clusters have more bonds per molecule than ice, have very little strain energy, and hence require lower energies of formation. The large clathrates ($n>70$) have considerable strain

energy[19] and are unlikely to contribute significantly to the partition function for large values of n. For water clusters with $n>70$, the most probable structure is a combination of five- and six-membered rings with the latter predominating with increasing n and eventually determining the structure of the macroscopic ice crystal. We have also shown in Fig. 6 the liquid drop model (uncorrected for translation and rotational energy of the center of mass of the cluster[20]) and a "spherical ice cluster" model. The latter is identical to the liquid drop model except for the use of ice surface tension[21] rather than liquid water surface tension in the energy of formation. This spherical ice cluster model was used to indicate what relation, if any, its nucleation rates had to those for the ice I_h molecular model. It was not considered seriously as a good model for vapor–ice nucleation.

The experimental points in Fig. 6 correspond to an initial cloud chamber temperature of 25 °C. The final temperatures for the experimental points range from 269 K at $S=5.4$ to 266 K at $S=6.5$. Since these relatively high temperatures are not expected to produce direct nucleation of ice from the vapor, we present in Fig. 7 results from calculations using a lower starting temperature, 3 °C. The figure contains one experimental point[22] and gives results of our calculations for ranges of S and T which will be studied further by Anderson, Miller, and Kassner.[22]

Homogeneous nucleation rates for water or ice from a supersaturated vapor are difficult to obtain experimentally. A simpler check on the theory has been to measure the critical supersaturation ratio as a function of temperature.[23] In our calculations, we define the critical supersaturation ratio, S_C, to be that value of S which produces a homogeneous nucleation rate of one drop per second per cubic centimeter. Since J is very
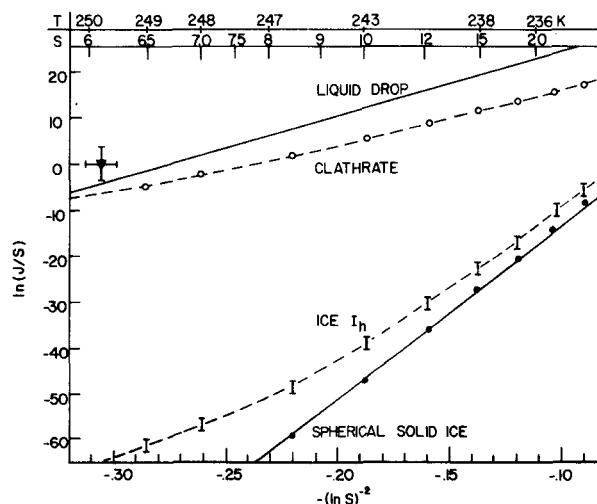

FIG. 7. The calculated $\ln(J/S)$ are shown vs $(-\ln S)^{-2}$ for the ice I_h, the clathrate, the liquid drop, and the spherical ice cluster models corresponding to experimental values of T and S obtained with an initial cloud chamber temperature of 3 °C. One experimental point from the work of Anderson and Miller[22] is shown (∇).
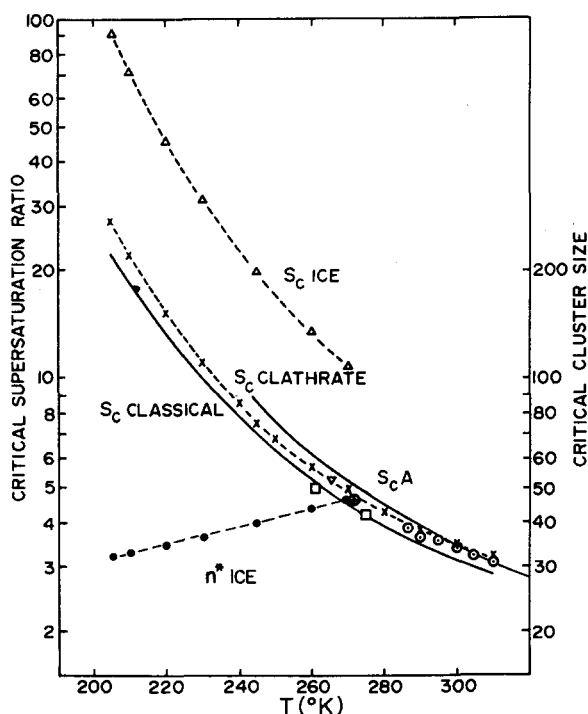
FIG. 8. The critical supersaturation ratios (with respect to water) are plotted as a function of temperature for the ice $I_h(\triangle)$ and clathrate[2] ($\times$) molecular models. The critical size ice I_h cluster is also shown for T and $S = S_c$. The experimental points are: $\square$, Volmer and Flood[23]; $\oplus$, Kassner et al.[18]; $\circ$, Heist and Reiss[25]; $\triangledown$, Anderson et al.[22] The solid line ($S_c A$) gives critical supersaturation ratios calculated by Abraham[24] using Wegland's gas model of a cluster.

sensitive to the value of S ($J \simeq S^{n*}$), S_C is coincident with the plainly visible onset of nucleation. Figure 8 shows S_C for the ice I_h model and for the clathrate model as a function of temperature. The figure also gives the critical-sized ice I_h cluster and some experimental points by Volmer and Flood[23] and Biermann and Kassner.[18] For further comparison, we have included in Fig. 8 critical supersaturation ratios calculated with Abraham's empirical $w(g)$ model.[24] This model gives results which are very close to those obtained by the molecular model using clathrate structures for temperatures around 290 K. However Abraham's model gives over-all nucleation rates which are 10^4 too small for water and S_C which are lower than the molecular model above 300 K and are higher below 290 K. Anderson, Miller, and Kassner[22] have made some recent measurements for S_C at $T = 250$ K, 255 K, 260 K, and 265 K which agree well with the clathrate model results at 255 K and above. Below $T = 255\,°$K, the trend is still unclear. The S_C may begin falling off from all model calculations with a very small slope—much the same as in the results compiled and reported by Pound et al.[3] The critical supersaturation ratios calculated for the ice I_h and clathrate models for temperatures less than about 240 K should be viewed with some caution. The nucleation rate is sensitive to the temperature dependence of the equilibrium vapor pressure for ice (or water) and at low temperatures data on vapor pressure are scarce. We have used an extrapolation formula[26] to

determine ice and water vapor pressure below 273 K. A second problem is the temperature dependence of librational frequencies for temperatures differing significantly from 273 K. An increase in these frequencies with decreasing T would increase the energy of formation and predict lower critical supersaturation ratios than those given in Fig. 8.

IV. SUMMARY AND CONCLUSIONS

The molecular model[1,2] has been applied specifically to ice I_h clusters in a supersaturated vapor in order to study the nucleation rates and critical supersaturation ratios of the vapor-to-ice nucleation process. The results indicate that direct homogeneous nucleation from the vapor to ordinary ice is extremely improbable for a large range of temperatures and supersaturation ratios: $T > 210$ K and $S < 20$. Further extensions of the molecular model to lower T and larger S are not realistic without more information about the temperature dependence of librational frequencies and a more reliable method of calculating equilibrium vapor pressures at low temperatures. Comparison with previous work using the molecular model[1,2] strongly suggests that small (less than 60 molecules) solidlike water clusters prefer a more spherical configuration (such as the clathrates) rather than the structure associated with the bulk ice.

The most significant results of this study are the large differences between the supersaturation ratios and the nucleation rates obtained for ice I_h and those obtained for clathrate clusters (see Figs. 6–8). These not only demonstrate the small probability for direct vapor-to-ice nucleation, but also illustrate the ability of the molecular model to reflect the effect of molecular environment and differences in cluster structure. The comparison of the two structures was made using the *same* librational frequencies, intramolecular frequencies, intermolecular force constants, hydrogen bond energies, and counting procedure for $\Omega(n)$. The absolute numbers for $\Delta\phi(n)/kT$ (and J) may be disputed on the grounds that $\Delta\phi(n)/kT$ is very sensitive to the bond energies, E_i, and to a lesser extent to the other quantities. The sensitivity of the free energy of formation to these parameters has led to reservations about the numerical values of predicted nucleation rates. Agreement with experiment has been good,[2] but the possibility of compensating errors or coincidence exists. However the comparison of results for the two different $(H_2O)_n$ structures using the same parameters should be valid and the observed differences meaningful.

A second rather unexpected result of this work is the qualitative (and quantitative) agreement between the molecular model calculations and the corresponding capillarity approximations. It was certainly not obvious a priori that a solid spherical cluster with the surface tension and density of bulk ice would predict energies of formation which approximately agree with the molecular model. This spherical ice model suffers from all the inadequacies of the liquid drop (Becker–Doring[27]) model for vapor-to-liquid homogeneous nucleation. Neither account for the translation and rotation of the center of mass of the cluster as pointed out by Lothe and Pound,[28]

and both models use macroscopic surface tension to calculate the energy required to form the surface of very small clusters. Recently Lee, Abraham, and Pound[29] have shown that for solid (fcc) spherical clusters of atoms (such as argon) the capillarity approximation overestimates the number of surface atoms and at the same time underestimates the surface free energy per surface atom. These compensating errors result in the fortuitous qualitative success of the simple uncorrected liquid (or solid) drop model.

A complete molecular model description for water of the vapor-to-liquid or vapor-to-solid homogeneous nucleation process will require a thorough investigation of competing structures and their contribution to $Z_c(n)$. In our previous work[2] fair agreement with experiment was obtained using only one type of clathrate structure—contributions from distorted clathrates or those composed of mixtures of five- and six-membered rings were not included. Probably the best explanation for the success of the five-membered ring clathrate structure is that it dominates the sum [Eq. (3)] over the possible states in the canonical partition function because of its large binding energy (and low energy of formation). Other configurations with higher energies of formation undoubtedly exist with the cluster structure fluctuating. This configurational entropy is important. However there is no reason to believe that (for the vapor-to-liquid process) it need be as large as the configurational entropy of an equal number of molecules in the bulk liquid. Collision rates are smaller in the vapor and the molecules have fewer positions they can occupy and still remain a part of the cluster. There are no obvious criteria for demanding that the small cluster be "liquid," and the true structure for small clusters could be anywhere between liquidlike and ordered microcrystalline. At the present time it is not possible to further characterize the clusters other than to observe the success of the molecular model, with specific postulated structures, to predict experimental quantities such as nucleation rates and critical supersaturation ratios.

In summary, these results for the homogeneous nucleation of ice clusters from a supersaturated vapor together with similar previous studies for clathrates[1,2] have shown that including the effects of molecular environment and specific cluster structures is possible. Moreover in the molecular model the conceptual difficulties and omissions of the classical theories are avoided. While the structures we have studied are not a complete description of the prenucleation water clusters, the agreement with experiment indicates that important features of these clusters have been accounted for. Extension of the model to describe the heterogeneous nucleation process is in progress and preliminary results[30] are encouraging. It now appears feasible to attempt molecular modeling of the more complex processes which occur under actual atmospheric conditions.

ACKNOWLEDGMENTS

*Work supported in part by the Atmospheric Sciences Section, National Science Foundation, GA 32386.

[1]P. L. M. Plummer and B. N. Hale, J. Chem. Phys. 56, 4329 (1972).

[2]B. N. Hale and P. L. M. Plummer, J. Atmos. Sci. 31, 1615 (1974).

[3]G. M. Pound, L. A. Madonna, and C. M. Sciulli, Conference on Nucleation, p. 85 (1953).

[4]J. A. Pople, D. L. Beverage, and P. A. Dobosh, J. Chem. Phys. 47, 2026 (1967).

[5]P. L. M. Plummer, Bull. Am. Phys. Soc. 16, 696 (1972).

[6]P. L. M. Plummer, in Physics and Chem. of Ice, edited by E. Whalley, S. J. Jones, and L. W. Gold (Royal Society of Canada, Ottawa, 1973), p. 109.

[7]J. H. Schachneider, Shell Tech. Repts. No 2. 231–64 (1964) and 57–65 (1965), Shell Develop. Co., Emeryville, CA.

[8]D. Eisenberg and W. Kauzmann, The Structure and Properties of Water (Oxford, New York, 1969); N. H. Fletcher, The Chemical Physics of Ice (Cambridge U. P., London, 1970).

[9]J. E. Bertie and E. Whalley, J. Chem. Phys. 46, 1264 (1967).

[10]W. C. Hoover, A. C. Hindmarsh, and B. L. Holian, J. Chem Phys. 57, 1980 (1972); F. F. Abraham, R. N. Kortzeborn, and H. H. Wang, IBM Res. Rept. RF-1114 (1972); F. F. Abraham, Homogeneous Nucleation Theory (Academic, New York, 1974).

[11]W. F. Giauque and J. W. Stout, J. Am. Chem. Soc. 58, 1144 (1936).

[12]G. Nemethy and S. A. Scheraga, J. Chem. Phys. 36, 3382 (1962), Table II.

[13]W. G. Courtney, J. Chem. Phys. 56, 2018 (1962) and references contained therein.

[14]R. M. Koros, J. M. Deckers, and Michel Boudart, "Sticking Probability of Water on Ice," Proceedings of the International Symposium on Condensation and Evaporation of Solids, Dayton, OH (Gordon and Breach, New York, 1964), p. 681. A value of $\alpha = 0.83 \pm 0.12$ for water on ice was reported.

[15]Several different forms for $\Delta\phi/kT$ were tried and the nucleation rate was calculated with Eq. (23). Variations in J were less than an order of magnitude and for the most part a factor of 2 or 3.

[16]J. B. Zeldovich, Sov. Phys. JETP 12, 525 (1942); Acta Phys. Chem. USSR 18, 1 (1943).

[17]A. H. Biermann, Ph. D. dissertation, University of Missouri-Rolla, 1972.

[18]The experimental points (for a helium filler gas) are taken from Fig. 3 of J. L. Kassner, Jr., P. L. M. Plummer, B. N. Hale, and A. H. Biermann, Proceedings of the International Weather Modification Conference, Canberra, Australia (American Meteorological Society, Boston, 1971), p. 51. For Fig. 6 the assumption was made that only the points above the "knee" of Biermann's curve correspond to true homogeneous nucleation. Biermann[17] gives a discussion of the interpretation of the points below the knee. The uncertainty shown in the points for the lower supersaturations represents only the uncertainty in the heterogeneous component which was subtracted out in order to obtain the homogeneous nucleation rate. At higher supersaturations, these uncertainties are insignificant.

[19]D. E. Hagen, Bull. Am. Phys. Soc. 18, 609 (1973).

[20]Jens Lothe and G. M. Pound, J. Chem. Phys. 36, 2080

(1962).

[21]The surface tension for the ice–vapor surface was taken to be $141-0.15T$ erg/cm^2 (where T is in degrees Kelvin). A value of about 100 erg/cm^2 at $T = 0$ °C is suggested by N. H. Fletcher, *The Physics of Rainclouds* (Cambridge U. P., Cambridge, England, 1966), p. 215. A. V. S. de Reuck, Nature 179, 1119 (1957) gives a value of about 116–119 erg/cm^2 at -38 °C and [σ ice vapor $-$ σ water vapor] = 28 at 0 °C (and 32 at -38 °C). From this one can estimate σ ice–vapor $\simeq 106$ ergs/cm^2 at 0 °C.

[22]Rodney Anderson, Ronald Miller, and James L. Kassner, Jr., University of Missouri-Rolla, Rolla, MO (unpublished).

[23]M. Volmer and H. Flood, Z. Physik. Chem. (Leipz.) 170, 273 (1934); K. C. Russell, J. Chem. Phys. 50, 1809 (1969); see also L. B. Allen and J. L. Kassner, Jr., J. Colloid Interface Sci. 30, 81 (1968) and discussion by Jens Lothe and G. M. Pound, *Nucleation*, edited by A. C. Zettlemoyer (Dekker,

New York, 1969), Chap. 3, pp. 119–120.

[24]Farid F. Abraham, J. Appl. Phys. 36, 4791 (1968).

[25]R. H. Heist and H. Reiss, J. Chem. Phys. 59, 665 (1973).

[26]E. W. Washburn, *International Critical Tables, National Research Council*, (McGraw-Hill, New York, 1928), Vol. III, p. 210–212; *Smithsonian Meteorological Tables* (The Smithsonian Institution, Washington, D. C., 1951), 6th revised ed., p. 350.

[27]R. Becker and W. Doering, Ann. Physik 24, 719 (1935).

[28]Jens Lothe and G. M. Pound, J. Chem. Phys. 36, 2080 (1962).

[29]Jong K. Lee, Farid F. Abraham, and G. M. Pound, Surface Sci. 34, 745 (1973).

[30]P. L. M. Plummer and B. N. Hale, Proceedings of the VIII International Conference on Nucleation, Leningrad, USSR, September, 1973, and P. L. M. Plummer and B. N. Hale (unpublished).